Available online at www.sciencedirect.com

ScienceDirect

Procedia Manufacturing 44 (2020) 425–432

Procedia MANUFACTURING

www.elsevier.com/locate/procedia

1st International Conference on Optimization-Driven Architectural Design (OPTARCH 2019)

Structural optimization of elastic circular arches and design criteria

Francesco Trentadue[a], Alessandra Fiore[a,]* , Rita Greco[b], Giuseppe C. Marano[c] and Nikos D. Lagaros[d]

[a]*Politecnico di Bari, DICAR, Via Orabona 4, 70125 Bari, Italy*
[b]*Politecnico di Bari, DICATECh, Via Orabona 4, 70125 Bari, Italy*
[c] *Politecnico di Torino, Corso Duca degli Abruzzi 24, 10129 Torino, Italy*
[d]*Institute of Structural Analysis and Antiseismic Research, School of Civil Engineering, National Technical University Athens, Heroon Polytechniou St. 9, Athens 15780, Greece*

Abstract

Even if arches represent an old structural system adopted in construction practice since two thousand years ago, they are still adopted just if large spans have to be covered. The structural efficiency of arches principally depends on optimal material exploitation, due to the minimization of the thrust curve eccentricity, which reduces structural material volume and weight. Although the millenarian use and a very abundant literature dealing with arches, there is still scope for design optimization, so this study is framed within this context, investigating plane circular arches under uniformly distributed vertical load and self-weight. The arches are simply supported with bending springs at end sections. In a first step an analytical solution of the arch static is derived in dimensionless form. Next, the volume of the arch is minimized. Finally, the results are charted to allow their use in a design process.

Peer-review under responsibility of the scientific committee of the 1st International Conference on Optimization-Driven Architectural Design

Keywords: arch; bending springs; force method; volume minimization.

* Corresponding author. Tel.: 0039-0805963876.
E-mail address: alessandra.fiore@poliba.it

2351-9789
Peer-review under responsibility of the scientific committee of the 1st International Conference on Optimization-Driven Architectural Design
10.1016/j.promfg.2020.02.274

1. Introduction

Arches are inherently efficient structures; they are capable to transfer loads from the superstructure to the foundations [1] with low structural weight. If properly shaped, they become the optimal solution to cross large spans and transfer high loads. Structural efficiency depends on the predominance of axial internal forces with low eccentricity [2-4]: in this circumstance smaller cross sections can be used with respect to beams. Contrarily, large eccentricities of axial internal forces or large shear stresses lead to uneconomical design, sub-exploitation of building materials and unnecessary self-weight [5,6]. Further design economy can be achieved via a more demanding overall shape optimization, aimed at satisfying specific objectives and constraints. In many cases structural volume is minimized.

From the data of 55 arch bridges built during the twentieth century reported in [7], several empirical lessons may be learnt. The first one is that (longer span) concrete arches require, per unit length, higher material quantities as compared to (shorter span) post tensioned concrete girder bridges. This is an expected result, at least since arches are curved, whereas beams are not and, moreover, post tensioned concrete girders are not usable on large spans. The second lesson is that, for long span arch bridges, arch self-weight is about half of the total vertical load. Both lessons motivate the search for optimal (less material consuming) solutions.

Traditionally, it is since the 17th century that firstly Galileo and next Hooke approached the hanged chain problem, but more accurate solutions, published on Acta Eruditorum, are due to Bernoulli, Leibniz and Huygens. Since then, the catenary curve has been addressed as optimal solution for compressive arch ribs under directly applied loads, or for suspended cables in tension. Catenary arches show properties of pure compression, without bending moment or shear stress. A chain suspended between two points will form this curve, which is routinely used for arches, and sometimes for shells (although this is not fully correct due to bidimensional stiffness). It is worth to remember that Hooke, as reported by Heyman, was the first experimentalist; he introduced the concept of inverted catenary as optimal arch form. Significant support was also given by Gaudí, Otto and Isler during the 19th and 20th century. These traditional studies focused on the hanged chain problem mainly regarded masonry arches in which opening of joints between vassoirs and sliding at interfaces must be avoided.

Another more recent approach is focused on the search of the optimal shape of arches modeled as elastic structures. In this context, a very interesting study on moment-less arches was proposed by Lewis [13]. In his mathematical model, a prediction on a simply supported arch rib shape is presented. Both arch self-weight and a uniformly distributed load are included in the analysis in order to show which geometry, among parabolic or catenary arch, is the most suitable one. Results show that catenary arch shape produces lower stresses.

Another very recent analytical study about arch configuration is due to Osserman [14]; he clarifies in a precise and mathematical fashion the motivations of the Gatway Arch shape in St. Louis.

A challenging view on these results can be also found in Tyas et al. [15] where it is proved, by numerical evidences, that a parabolic funicular is not necessarily the optimal structural form to carry a uniform load between fixed supports; so an explicit analytical expression for geometry and stress is proposed in order to design suitable truss systems emerging from the supports and thus obtain a global optimization.

A fresh look upon optimization approach is also presented in the study by Vanderplaats and Han [16], where an optimization technique based on an iterative force approximation method is combined with a finite-element technique to obtain a minimum arch volume, by assuming variable cross-section. Further studies have been performed, for both buildings and bridges in [8-11] and [17, 18].

This study is focused on the optimal design of an elastic plane circular arch having fixed span L, uniform cross section and subjected to a uniform vertical load and to its self-weight. We assumed that the only non-null deformation is the bending curvature. Although the obtained results are not framed in a general context, they allow us to highlight the main variables governing the problem and are useful for predesign purposes.

2. Problem statement

In Fig.1a the static scheme of the right half of a circular arch of radius R is represented, in which ϑ is the colatitude of a generic section and β the colatitude of the end section.

Intermediate condition between hinged and clamped supports are considered, i.e. bending springs of stiffness K are applied at end sections (Fig. 1a).

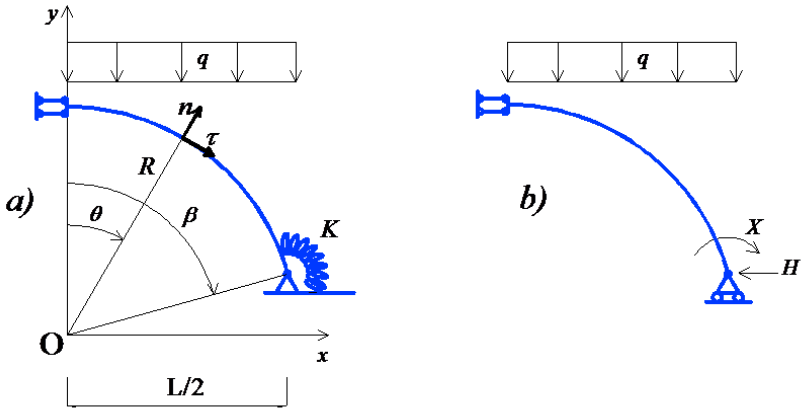

Fig.1: a) Static scheme. b) Primary structure in force method.

The arch has a uniform cross section area A, is made up of a homogeneous material with specific gravity weight γ and is subjected to its self-weight and to a uniformly distributed vertical load for unit horizontal length q. So the tangent load p_τ and normal load p_n for unit length of arch are given by

$$\begin{cases} p_\tau = (q cos\vartheta + \gamma A)\sin\vartheta \\ p_n = -(q cos\vartheta + \gamma A)\cos\vartheta \end{cases} , \tag{1}$$

where the unit vectors $\boldsymbol{n}$ and $\boldsymbol{\tau}$ are shown in Fig. 1a and $qcos\theta$ is the applied vertical load for unit length of arch. The equilibrium equations can be written as

$$\begin{cases} N'(s) + \frac{T(s)}{R} = -\left[\gamma A \sin\left(\frac{s}{R}\right) + \frac{1}{2} q \sin\left(\frac{2s}{R}\right)\right] \\ T'(s) - \frac{N(s)}{R} = \left[\gamma A cos\left(\frac{s}{R}\right) + q cos^2\left(\frac{s}{R}\right)\right] \\ M'(s) + T(s) = 0 \end{cases} , \tag{2}$$

where: $s=\theta R$; N is the axial internal force; T is the shear internal force and M is the bending moment.
Togheter with the above equations, the following boundary conditions must be fulfilled

$$\begin{cases} T(0) = 0 \\ N(0) = -H \\ M(\beta) = -X \end{cases} , \tag{3}$$

where X and H are the horizontal thrust and the negative bending moment at the end sections, which will be considered redundant forces. The following dimensionless mechanical variables are now introduced:

$$n = \frac{N}{qL};\ t = \frac{T}{qL};\ m = \frac{M}{qL^2};\\ \mu = \frac{\gamma A}{q};\ h = \frac{H}{qL};\ x = \frac{X}{qL^2} . \tag{4}$$

and the geometric relation

$$\frac{R}{L}=\frac{1}{2\sin(\beta)} \tag{5}$$

is also considered. Equations (1-5) allow us to derive the dimensionless internal forces n, t and the dimensionless bending moment m as follows:

$$n(\vartheta,\beta,h)=\frac{1}{2}\big(-2h\cos(\theta)-\csc(\beta)\sin(\theta)\,(\theta\mu+\sin(\theta))\big); \tag{6a}$$

$$t(\vartheta,\beta,h)=\frac{1}{2}\big(-2h\sin(\theta)+\csc(\beta)\cos(\theta)\,(\theta\mu+\sin(\theta))\big); \tag{6b}$$

$$\begin{aligned} m(\vartheta,\beta,h,x)=\frac{1}{8}(&-8x-\cot(\beta)^2+2(\beta\mu-2h\cos(\theta))\csc(\beta)+2\cot(\beta)(2h+\mu\csc(\beta))\\ &+\csc(\beta)^2(-2\mu\cos(\theta)+\cos(\theta)^2-2\theta\mu\sin[\theta])). \end{aligned} \tag{6c}$$

Next, to determine the dimensionless redundant forces x and h, the Force Method is applied. As already stated, the curvature κ is assumed as the only non-null deformation, expressed by:

$$M=EJ\kappa\ . \tag{7}$$

The primary structure is shown in Fig. 1b and the compatibility conditions $u_x(B)=0$ and $\gamma(B)+X/k=0$ are imposed, where $u_x(B)$ and $\gamma(B)$ are the horizontal displacement and the rotation at the end section B.
Then, by means of virtual force theorem, the two compatibility conditions lead to the system of simultaneous equations:

$$\begin{cases} \dfrac{L}{2sin\beta}\displaystyle\int_0^\beta \frac{m_h\,m}{EJ}d\theta=\dfrac{L}{2sin\beta}\displaystyle\int_0^\beta \frac{m(\vartheta,\beta,1,0)\,m(\vartheta,\beta,h,x)}{EJ}d\theta=0\\ \dfrac{L}{2sin\beta}\displaystyle\int_0^\beta \frac{m_x\,m}{EJ}d\theta=\dfrac{L}{2sin\beta}\displaystyle\int_0^\beta \frac{m(\vartheta,\beta,0,1)\,m(\vartheta,\beta,h,x)}{EJ}d\theta=-\dfrac{x}{k} \end{cases}, \tag{8}$$

where $k=KL/EJ$ is the dimensionless stiffness of the springs; m is given by Eq.(6c); m_h is the dimensionless bending moment due to a unit thrust and $m_x=-1$. The dimensionless redundant forces x and h are thus determined by solving Eqs. (8):

$$\begin{aligned} x=-((&k\csc(\beta)^2(27-36(1+4\beta^2)\mu\cos(\beta)+8(-4+3\beta^2)\cos(2\beta)+36\mu\cos(3\beta)+5\cos(4\beta)\\ &+252\beta\mu\sin(\beta)-96\beta^3\mu\sin(\beta)-28\beta\sin(2\beta)+12\beta\mu\sin(3\beta)+2\beta\sin(4\beta)))/(192(-2k+\\ &-2k\beta^2 3\cos(\beta)+\ 2k\cos(2\beta)+3\cos(3\beta)+6\beta\sin(\beta)+k\beta\sin(2\beta)+2\beta\mathrm{Sin}(3\beta))) \end{aligned} \tag{9a}$$

$$\begin{aligned} h=(&\csc(\beta)(9+48k\mu-24k\beta^2\mu-3(k+2(-9+4\beta^2)\mu)\cos(\beta)\\ &+4(-4+3k(-4+\beta^2)\mu)\cos(2\beta)+3k\cos(3\beta)-54\mu\cos(3\beta)+\\ &24\beta^2\mu\cos(3\beta)+7\cos(4\beta)+6k\beta\sin(\beta)-36\beta\mu\sin(\beta)-42k\beta\mu\sin(2\beta)+\\ &2k\beta\sin(3\beta)-60\beta\mu\sin(3\beta))+\ \ 6\beta\mathrm{Sin}(4\beta)))\,/(24(-2k+2k\beta^2-3\cos(\beta)+\\ &2k\cos(2\beta)+3\cos(3\beta)+6\beta\sin(\beta))+k\beta\sin(2\beta)+2\beta\sin(3\beta))) \end{aligned}\ . \tag{9b}$$

3. Optimal solution

The optimal shape that minimizes the arch volume is herein searched. In each section the stress under axial-bending condition must satisfy the constraint:

$$\sigma_{\max} = \left|\frac{M}{W} + \frac{N}{A}\right| = \frac{qL}{A}\left(\frac{LA}{W}|m| - n\right) \leq f_d \tag{10}$$

where W is the section modulus; f_d is the design strength of the material and the dimensionless axial force n and the dimensionless bending moment m are given by Eqs. (6) and (9). In (10) it has been considered that n is always negative. For the structural scheme under examination it is not possible to determine a priori in which section the stress σ_{max} reaches its maximum value. To highlight this circumstance in Fig.2 the dimensionless moment m is drawn. We notice that for small values of k (in the range 1-10) the maximum bending moment is attained in correspondence of an internal section, while for high values of k (>10) it is attained at end sections (Fig. 2).

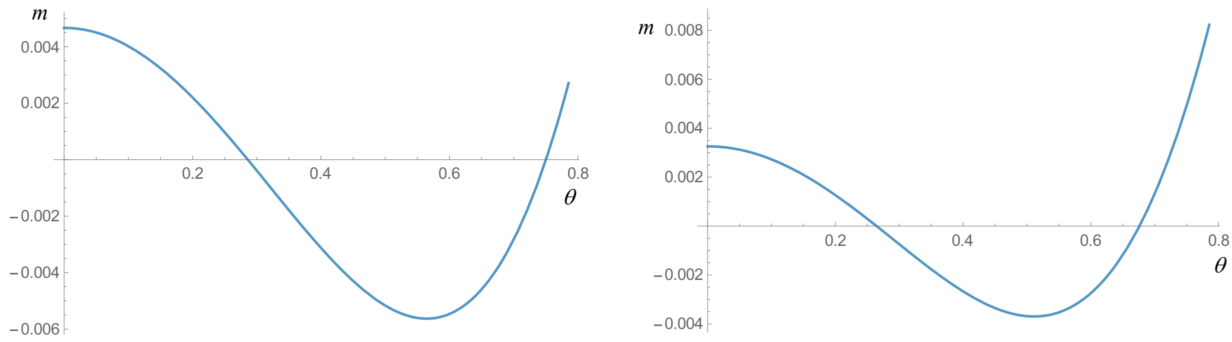

a) *b*)

Fig. 2 Function m versus θ for $\beta=\pi/4$ and $\mu=1$: *a*) $k=5$; *b*) $k=500$.

As a result, the cross section area A must be determined as

$$A = \max_{0\leq\vartheta\leq\beta} \frac{qL}{f_d}(-n + \lambda|m|) \tag{11}$$

where λ is a slenderness parameter, defined as $\lambda = AL/W$. For instance, in case of rectangular section, we have $\lambda = 6L/h$, where h is the height of the section. Eq. (11) cannot be directly solved since the dimensionless axial force n and the bending moment m depend on the cross-section area A through the parameter μ, defined in Eq. (4). To overcome this drawback, the dimensionless internal forces are written as

$$\begin{aligned} n &= n_q + \mu n_\mu \\ m &= m_q + \mu m_\mu \end{aligned} \tag{12}$$

and the dimensionless span $\eta = \gamma L/f_d$ is introduced. Since we have

$$\mu = \eta \frac{Af_d}{qL} , \tag{13}$$

Eq. (11) becomes

$$A(\beta,\lambda,\eta)=\frac{qL}{f_d}\max_{0\le\vartheta\le\beta}\frac{-n_q+\lambda|m_q|}{1-\eta(-n_\mu+\lambda|m_\mu|)} \quad . \tag{14}$$

In (14) it has been considered that n_q and n_μ are always negative. Since it is no possible to obtain a closed-form solution for Eq. (14), the minimum feasible cross section area $A(\beta,\lambda,\eta)$ must be searched numerically. The above introduced dimensionless span η has a clear mechanical interpretation: it is the ratio between the arch span L and the height $\bar{h}=f_d/\gamma$ of a column made by the same material of the arch, subjected to its self-weight, in which at the base section the design stress f_d is attained. In view of Eq. (5) the volume V can be finally obtained as

$$V(\beta,\lambda,\eta)=A(\beta,\lambda,\eta)\frac{L\beta}{\sin\beta}=\frac{qL^2}{f_d}\frac{\beta}{\sin\beta}\max_{0\le\vartheta\le\beta}\frac{\left(-n_q+\lambda|m_q|\right)}{\left(1-\eta(-n_\mu+\lambda|m_\mu|)\right)} \tag{15}$$

The obtained result is shown in Fig.3, in which the dimensionless volume f_dV/qL^2 is drawn versus the rise to span ratio

$$\frac{f}{L}=\frac{1-\cos\beta}{2\sin\beta} \tag{16}$$

A fixed value λ =600 of the slenderness parameter is firstly considered, whereas the dimensionless span takes the values η ={0.1, 0.2, 0.3, 0.4, 0.5} and the dimensionless spring stiffness is set equal to k ={0, 10, 50, 500}.

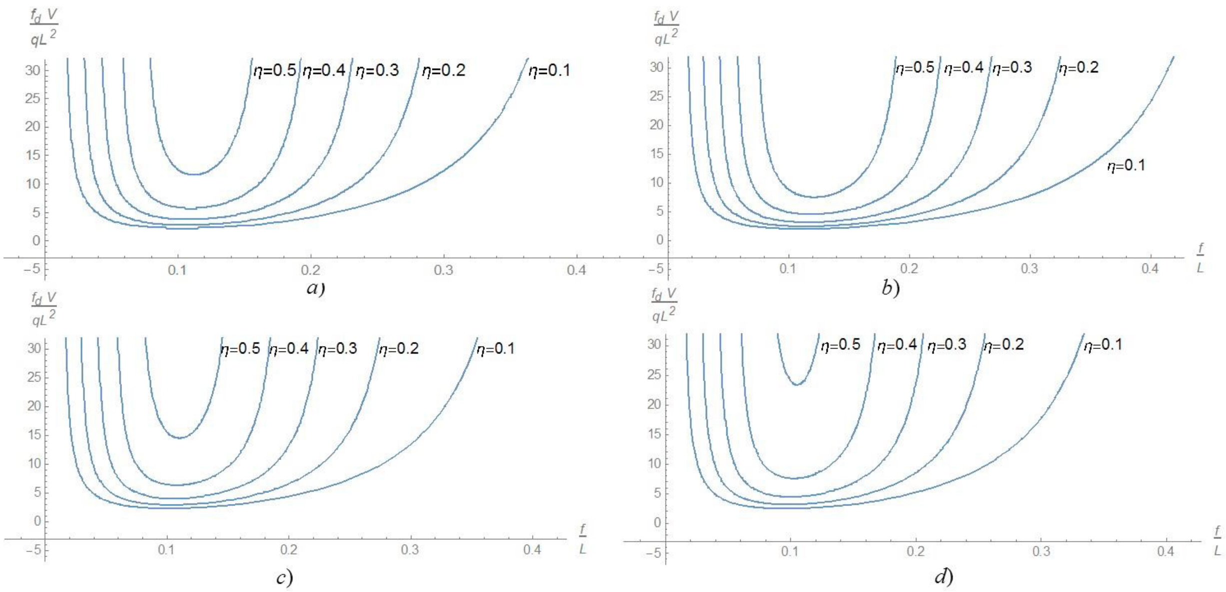

Fig. 3 Function (f_dV/qL^2) versus f/L for λ=600: a) k=0; b) k=10; c) k=50; d) k=500.

It emerges that, for all curves, the values of f/L in the range [0.1, 0.15] produce the best values of the dimensionless volume f_dV/qL^2 . It is worth to remark that this range of optimal values of f/L is independent from the applied load q and from the span L . The graphs also show that, as expected, the dimensionless span η strongly influences the value of the optimal dimensionless volume, so it results a fundamental parameter governing the design. In fact, in view of Eq. (15), the dimensionless volume tends to infinity when in a generic section we have

$$\left(-n_\mu+\lambda m_\mu\right)\to\frac{1}{\eta} \quad . \tag{17}$$

It could be shown that when Eq. (17) holds, the condition $\sigma_{max}=f_d$ is immediately attained yet for a null value of q, as a effect of the self-weight only. More specifically, we can find a range of feasible values of the rise to span ratio f/L for each set of values of η, λ and k. At the boundaries of this range the dimensionless volume tends to infinity, regardless the value of the external load q. As it can be inferred from Figs. 3 and 4, the main variable determining this range is the dimensionless span η. As expected, by increasing the dimensionless span η the range of feasible values for the dimensionless rise f/L tends to narrow and the minimal dimensionless volume increases. In Fig, 4 the same graphs of Fig. 3 are derived for λ=200. As expected, design solutions with low slenderness lead to lower values of the minimal dimensionless volume.

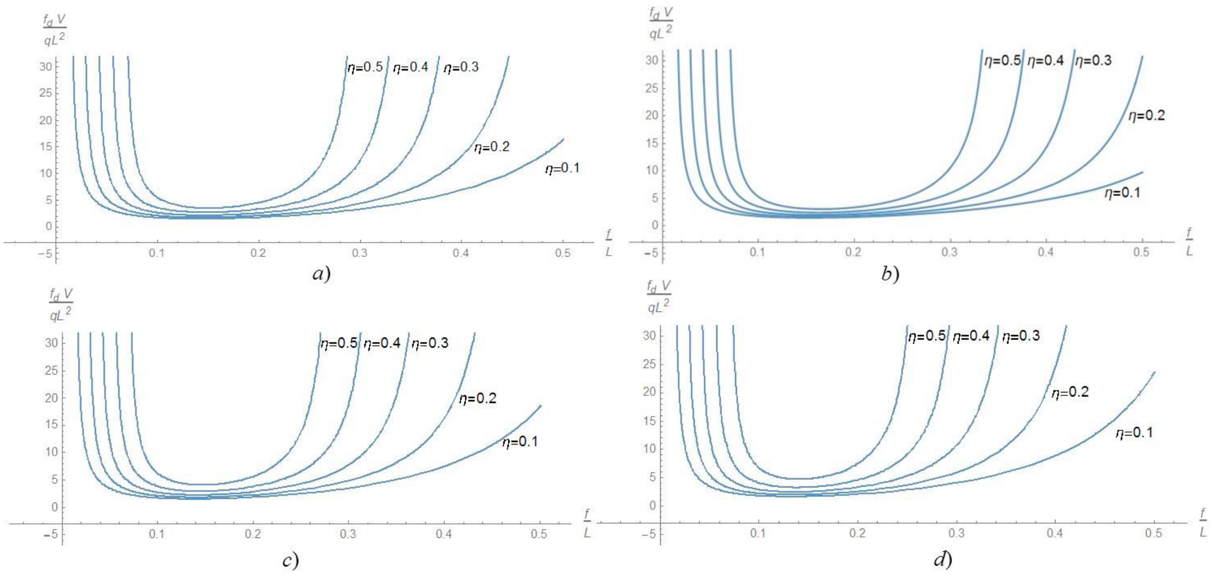

Fig. 4 Function (f_dV/qL^2) versus f/L for λ=200: a) k=0; b) k=10; c) k=50; d) k=500.

With regard to the influence of the dimensionless constraint stiffness k, from Figs. 3 and 4 it emerges that the best value of this parameter is about 10, so not corresponding neither to clamped ends or to simply supported ends. Finally, the following design procedure can be proposed based on the above graphs. First, the dimensionless span η is determined by the material properties γ, f_d and the span L. Next, the optimal values of the rise to span ratio f/L and of the dimensionless volume f_dV/qL^2 are evaluated by the graphs in Fig. 3 and Fig.4, for assigned values of λ and k.

The evaluation of the optimal volume V allows us on one side to estimate the cost of the structure and on the other to calculate the corresponding optimal cross-section dimensions. For example, in the case of rectangular cross-section, the height h and the width b could be obtained, after fixing the slenderness parameter λ, by the following relations:

$$h = \frac{6L}{\lambda}$$

$$b = V\lambda \frac{\sin\beta}{6L^2} \tag{18}$$

where the colatitude β can be determined by the dimensionless rise $\tilde{f}$ solving the equation

$$\frac{f}{L} = \frac{1-\cos\beta}{2\sin\beta} \tag{19}$$

which leads to a second-degree equation in the unknown $\cos\beta$.

4. Conclusions

In the present study a semi analytical solution for the optimal shape of a plane arch with bending springs at ends has been presented. Although the procedure is referred to the particular case of circular arches with uniform cross section, it allows to highlight the main variables governing the solution, in particular the dimensionless span and the rise to span ratio. Further, we have found that values of the rise to span ratio in the range [0.1, 0.15] in all cases here examined lead to a minimal weight, independently from the applied load q, from the span L and from the material properties.

Acknowledgements

The research study in the current paper has been conducted in the frame of the Research Funding Program: Marie Sklodowska-Curie Research and Innovation Staff Exchanges (RISE) "OPTARCH – Optimization Driven Architectural Design of Structures", H2020-MSCA-RISE-2015.

Reference

[1] A. Wilson, Practical Design of Concrete Shell. Monolithic Dome Institute, Texas, (2005).
[2] E. Allen and W. Zalewski, Form and Forces: Designing efficient, expressive structures. Wiley, (2009).
[3] G.C. Marano, F. Trentadue and F. Petrone, Optimal arch shape solution under static vertical loads, Acta Mechanica, 225(3) (2014) 679-686.
[4] C.Y. Wang and C.M. Wang, Closed-form solutions for funicular cables and arches, Acta Mechanica, 226(5) (2015) 16-41.
[5] M. Gohnert, A. Fitchett, I. Bulovic, and N. Bhikhoo, Structurally efficient housing using natural forms, J of the SAICE, 55(3) (2013) 96-102.
[6] D.P. Billington, Thin Shell Concrete Structures, McGraw-Hill, New York (1982).
[7] J. Salonga and P. Gauvreau, Comparative Study of the Proportions, Form, and Efficiency of Concrete Arch Bridges, Journal of Bridge Engineering, 19(3) (2014) 4013010.
[8] F. Trentadue, G.C. Marano, I. Vanzi, I. and B. Breseghella, Optimal arches shape for single-point-supported deck bridges, Acta Mechanica, 229 (2018) 2291–2297.
[9] A. Fiore, G.C. Marano, R. Greco, E. Mastromarino, Structural optimization of hollow-section steel trusses by differential evolution algorithm, International Journal of Steel Structures, 16 (2) (2016) 411-423.
[10] T. Zordan, B. Briseghella, E. Mazzarolo, Bridge Structural Optimization Through Step-By-Step Evolutionary Process, Structural Engineering International (SEI) 20(1) (2010) 72-78.
[11] R. Greco, G.C. Marano, A. Fiore, Performance-cost optimization of Tuned Mass Damper under low-moderate seismic actions, Structural Design of Tall and Special Buildings, 25 (18) (2016) 1103-1122.
[12] F. Trentadue, G. Quaranta, Limit analysis of frictional block assemblies by means of fictitious associative-type contact interface laws International Journal of Mechanical Sciences 70 (2013) 140-145.
[13] W.J. Lewis, Mathematical model of amoment-less arch, Proc. R. Soc. A, 472 (2016) 00-19.
[14] R. Osserman, How the Gateway Arch Got its Shape, Nexus Network Journal, 12 (2010) 167–189.
[15] A. Tyas, A.V. Pichugin, and M. Gilbert, Optimum structure to carry a uniform load between pinned supports: exact analytical solution, Proc. R. Soc. A, 467 (2011) 1101–1120.
[16] G.N. Vanderplaats and S.H. Han, Arch shape optimization using force approximation methods, Structural optimization, 2(4) (1990) 193–201.
[17] M. Gilbert, A. Tyas, Layout optimization of large-scale pin-jointed frames, Engineering Computations, 20(8) (2003) 1044-1064.
[18] D'Ambrosio P., De Tommasi D., Granieri L., Maddalena F., A surface energy approach to the mass reduction problem for elastic bodies, IMA Journal of Applied Mathematics, 74(6) (2009) 934-949.